Signals of additional Z' boson in $e^+e^- \to W^+W^-$ at the ILC with polarized beams

B. Ananthanarayan
Monalisa Patra

Centre for High Energy Physics
Indian Institute of Science
Bangalore 560 012, India

P. Poulose

Department of Physics
Indian Institute of Technology Guwahati
Assam 781 039, India

Abstract

We consider the possibility of fingerprinting the presence of heavy additional Z' bosons that arise naturally in extensions of the standard model such as E_6 models and left-right symmetric models, through their mixing with the standard model Z boson. By considering a class of observables including total cross sections, energy distributions and angular distributions of decay leptons we find significant deviation from the standard model predictions for these quantities with right-handed electrons and left-handed positrons at $\sqrt{s}$=800 GeV. The deviations being less pronounced at smaller centre of mass energies as the models are already tightly constrained. Our work suggests that the ILC should have a strong beam polarization physics program particularly with these configurations. On the other hand, a forward backward asymmetry and lepton fraction in the backward direction are more sensitive to new physics with realistic polarization due to interesting interplay with the neutrino t- channel diagram. This process complements the study of fermion pair production processes that have been considered for discrimination between these models.

1 Introduction

The International Linear Collider (ILC) is a proposed high energy, high luminosity electron-positron collider with the mission of studying the standard model (SM) at high precision and to look for signals beyond the standard model [1]. It has been proposed that an initial beam polarization program can also significantly enhance its capabilities in meeting these objectives, see ref. [2].

One of the important processes that will be studied at high precision at ILC with and without beam polarization [2] is W-pair production. Phenomenological studies of this process within the SM and some extensions have been carried out in great detail [3, 4] starting many years ago. Since properties of the weak gauge bosons are closely linked to electroweak symmetry breaking (EWSB) and the structure of the gauge sector in general, detailed study of W physics will throw light on what lies beyond the SM.

On the other hand, it is entirely likely that there are additional Z bosons, denoted by Z' in the TeV range, see for instance the review section in ref. [5]. These are present in several economical extensions of the standard model. With this strong motivation, signatures of such a gauge boson is searched for in the past and existing colliders. Direct and indirect searches at LEP as well as at TeVatron and other existing facilities provide bounds on the masses of this particle and on other model parameters. Direct searches at TeVatron put lower limits of $630-1030$ GeV [6, 7] and LEP 2 put limits of $673-1787$ GeV [8], while electroweak precision analysis of LEP provide lower limits of $475-1500$ GeV [9] on the mass, depending on the model considered. Even if not directly produced, they can be finger printed easily as they would mix with the traditional Z^0 of the electroweak model. Thus W-pair production process has a winning edge compared to fermion pair production when it comes to the effect of this mixing. This is because, as these Z' do not interact with the standard W bosons, the W-pair production process is insensitive to the presence of Z' in the absence of mixing. In contrast, fermion pair production process is sensitive to the presence of Z' even in the absence of mixing.

We note that although such mixing is highly constrained by precision measurements at LEP and by other existing experimental data [5], with the high statistics expected at the ILC for W-pair production, even such small mixing can be probed effectively. The new effects could be manifested in departures from the standard model cross section for W-pair production, and in various differential distributions and asymmetries.

Recently in the context of the littlest Higgs model(LHM), which also contain Z' bosons, we demonstrated the utility of several simple distributions in fingerprinting the model [10]. As a result, it may be worthwhile considering how other popular Z' models arising in E_6 unification and so called left-right symmetric models (LRSM) and alternative left-right symmetric models (ALRSM), which have also been considered by the CLIC Physics Working Group [11], can subject themselves to a diagnosis. This is the main aim of the present work. We have studied the process at reference energies of 500, 800 and 1000 GeV, and find that effects are pronounced only at the higher energy. In addition, we

conclude that initial beam polarization can significantly enhance the diagnostic ability of the ILC. In particular, for the class of models we are considering these effects are of importance for right-handed electrons and left-handed positrons in the process we are considering. This may be understood as arising from the dominant t-channel SM contribution which gets erased away with this choice of beam polarization revealing the new physics contributing through the s-channel. The above argument holds in the case for realistic degrees of polarization of the beams; it is expected that about 90% electron polarization would be achievable along with a positron polarization of 60% [2]. We present our results for both these cases and find that there are interesting effects even for the latter case as the t- channel contribution which now survives, can play an interesting and effective role.

We will use the observables considered by us in our earlier work, ref. [10], which are total cross sections, single energy distribution of the secondary lepton, lepton angular distribution and forward-backward (FB) and left-right (LR) asymmetries. In addition to the above we consider an important and useful energy-energy correlation of the type first considered in the context of some anomalous gauge couplings by Dicus and Kallianpur [12]. Despite its obvious utility it has not received much attention, and we will demonstrate how this correlation in combination with beam polarizations can extract important information on Z' models.

The scheme of this paper is the following: In Sec. 2 we discuss the details of the models we are considering. In Sec. 3 we consider the kinematics of the process and the subsequent decays in great detail. The section is organized in several subsections for convenience. In Sec. 4 we present a discussion including a comparison of W-pair production with fermion pair production considered in the literature, and our conclusions.

2 Z' Models

The presence of an additional neutral gauge boson (Z') is anticipated in many extensions of the SM. Some grand unified theories (GUT) like those based on E_6, which contain the gauge group of $SU(3)_C \times SU(2)_L \times U(1)_Y \times U(1)'$ clearly have additional $U(1)'$ symmetries (for a recent review, see, e.g. ref. [13]). These could also arise in superstring theories. There are many other extensions of the SM with dynamical symmetry breaking, Little Higgs models (LHM), LRSM and ALRSM also with extended gauge sectors. In models with large extra dimensions, Kaluza-Klein excitations of the SM gauge bosons propagating in the bulk manifest as extra gauge bosons in four dimensions. For our purposes we confine our attention to certain GUT models based on E_6 and LRSM and ALRSM. We will study the presence of an extra $U(1)'$ symmetry present in addition to the SM gauge symmetries, arising in the candidate models mentioned above. In some of these models there could be more than one neutral gauge bosons along with possible presence of heavy charged gauge bosons. We assume that any such additional gauge bosons decouple from the particle spectrum

under study, and therefore will be ignored in this study.

The new gauge boson Z' could mix with the SM gauge boson to give the physical eigenstates. As explained later in this section, the W-pair production in e^+e^- collisions has the advantage of directly probing the mixing unlike, for example, the fermion pair production process. This is because, the W does not interact directly with the Z'. While such mixing is highly constrained by the current experimental constraints, it may still be possible to probe its effect in a high energy, high luminosity machine like the ILC. With very high statistics expected for W-pair production at ILC, this process has the potential to probe even very small mixing permitted.

Let us now turn to some general features of the scenario. Here we closely follow the discussion in ref. [13, 14]. With one additional $U(1)'$ symmetry, the mass term of the neutral gauge bosons may be written as,

$$L_Z^{\rm mass} = \frac{1}{2}\begin{pmatrix} Z^{0\mu} & Z'^{\mu} \end{pmatrix}\begin{pmatrix} M_{Z^0}^2 & \Delta^2 \\ \Delta^2 & M_{Z'}^2 \end{pmatrix}\begin{pmatrix} Z_\mu^0 \\ Z_\mu' \end{pmatrix} \tag{1}$$

Diagonalizing the above mass matrix the mass term is presented in terms of the physical boson fields as

$$L_Z^{\rm mass} = \frac{1}{2}M_1^2\ Z_1^\mu Z_{1\mu} + \frac{1}{2}M_2^2\ Z_2^\mu Z_{2\mu}, \tag{2}$$

where we identify the lighter Z_1 as the observed Z-boson with $M_1 = 91.19$ GeV, and the Z_2 as its heavier counterpart. In terms of the SM gauge boson, Z_0 and the new gauge bosons, Z', we may write the physical states as

$$\begin{pmatrix} Z_1 \\ Z_2 \end{pmatrix} = \begin{pmatrix} \cos\theta & \sin\theta \\ -\sin\theta & \cos\theta \end{pmatrix}\begin{pmatrix} Z^0 \\ Z' \end{pmatrix}. \tag{3}$$

The mixing angle, θ is related to the diagonalization of the mass matrix, and can be expressed in terms of the physical masses and the SM mass parameter as

$$\tan^2\theta = \frac{M_{Z^0}^2 - M_1^2}{M_2^2 - M_{Z^0}^2}. \tag{4}$$

For our phenomenological analysis it is more convenient to re-parametrize the above by defining a mass difference $\Delta M = M_1 - M_{Z^0}$. Rearranging Eq. 4 the mass of the heavier gauge boson takes the form

$$M_2^2 = \frac{(1+\tan^2\theta)(M_1 - \Delta M)^2 - M_1^2}{\tan^2\theta}. \tag{5}$$

Thus, in our study we consider θ and ΔM as the two independent parameters of the mixing. The importance of mixing in W-pair production at ILC is clearly visible with the fact that the new gauge sector does not interact with the SM gauge sector directly, and therefore the W boson does not couple directly to Z' at tree level. Its couplings to the mass eigenstates Z_2 arises through mixing, along

with a corresponding weakening in its coupling to the lighter mass eigenstate, Z_1. These couplings are given by

$$g_{WWZ_1} = g_{WWZ^0} \cos\theta, \qquad g_{WWZ_2} = g_{WWZ^0} \sin\theta, \tag{6}$$

where g_{WWZ^0} is the SM coupling. Experimental constraints on the mixing limits the value of θ to be not larger than a few times 10^{-3}. At the same time, when the Higgs structure of the model is known, one may compute the mixing angle. In such a case, mixing angle can be expressed as

$$\theta = C \sqrt{\frac{5}{3}} \lambda \sin\theta_W \frac{M_{Z_1}^2}{M_{Z_2}^2}, \tag{7}$$

where λ is a parameter of order unity, C is function of the VEV's of the Higgs fields and their $U(1)'$ charges and θ_W is the usual Weinberg mixing angle. In Table 1 we present an illustrative case of E_6 models as discussed in Ref.[9]. The table also gives the mixing angle, θ and ΔM in each case corresponding to a representative value of $M_{Z_2} = 1$ TeV.

Model	C (range)	θ	ΔM (MeV)
$E_6(\chi)$	$\left[-\frac{3}{\sqrt{10}}, \frac{2}{\sqrt{10}}\right]$	$[-.0037, .0025]$	$[75, 33]$
$E_6(\psi)$	$\left[-\sqrt{\frac{2}{3}}, +\sqrt{\frac{2}{3}}\right]$	$[-.0032, .0032]$	56
$E_6(\eta)$	$\left[-\frac{1}{\sqrt{15}}, +\frac{4}{\sqrt{15}}\right]$	$[-.0010, .0040]$	$[6, 89]$
$LRSM$	$\left[-\frac{1}{\alpha_{LR}}\sqrt{\frac{3}{5}}, +\alpha_{LR}\sqrt{\frac{3}{5}}\right]$	$[-.0019, .0048]$	$[20, 124]$

Table 1: Mixing angle (θ) and ΔM corresponding to a Z_2 of mass 1 TeV in different models considered. The parameter in the left-right symmetric model (LRSM) takes a value, $\alpha_{LR} = \sqrt{1 - 2\sin^2\theta_W}/\sin\theta_W$.

We now turn our attention to the Zee coupling. The fermion couplings are highly model dependent. In the following we will very briefly describe this coupling in the models considered. A detailed analysis can be found in the literature including [13]. The neutral current interactions of electrons with the gauge bosons are given by the Lagrangian term,

$$\mathcal{L}_{NC} = J_{em}^{\mu} A_{\mu} + J_{SM}^{\mu} Z_{\mu}^0 + J'^{\mu} Z'_{\mu}, \tag{8}$$

where J_{em}^{μ} is the electromagnetic current with which the photon interact, J_{SM}^{μ} is the current with which the SM neutral gauge boson, Z^0 interact, and J'^{μ} is the current with which the new neutral gauge boson, Z' interact. In terms of the projection operators $P_{L,R} = (1 \mp \gamma^5)/2$ the currents take the form

$$J_i^{\mu} = -\bar{\psi}_e \gamma^{\mu} (g_{iL}^e P_L + g_{iR}^e P_R) \psi_e. \tag{9}$$

The SM couplings involved in J^{μ}_{SM} are expressed in terms of the Weinberg mixing angle, θ_W as

$$g^f_L = \frac{e}{\sin\theta_W \cos\theta_W}(-\frac{1}{2} + \ \sin^2\theta_W), \qquad g^f_R = \frac{e\sin\theta_W}{\cos\theta_W}. \tag{10}$$

Fermion couplings corresponding to the current, J'^{μ} in the cases of models considered in our study are tabulated in Table 2.

Model	g'^e_L	g'^e_R
$E_6(\chi)$	$\sqrt{\frac{3}{8}}\frac{e}{\cos\theta_W}$	$\sqrt{\frac{1}{24}}\frac{e}{\cos\theta_W}$
$E_6(\psi)$	$\frac{\sqrt{10}e}{12\cos\theta_W}$	$-\frac{\sqrt{10}e}{12\cos\theta_W}$
$E_6(\eta)$	$\frac{e}{6\cos\theta_W}$	$\frac{e}{3\cos\theta_W}$
$LRSM$	$\frac{e}{\cos\theta_W}\frac{1}{2\alpha_{LR}}$	$\frac{e}{\cos\theta_W}(\frac{1}{2\alpha_{LR}} - \frac{\alpha_{LR}}{2})$
$ALRSM$	$\frac{e}{\cos\theta_W \sin^2\theta_W}\frac{1}{\alpha_{LR}}(-\frac{1}{2} + \sin^2\theta_W)$	$\frac{e}{\cos\theta_W \sin^2\theta_W}\frac{1}{\alpha_{LR}}(-\frac{1}{2} + \frac{3}{2}\sin^2\theta_W)$

Table 2: $Z'ee$ couplings (Eq. 9) in different models considered. The parameter $\alpha_{LR} = \sqrt{1-2\sin^2\theta_W}/\sin\theta_W$.

In the next section, we will compare the effects found in the above models, with those arising in the Littlest Higgs scenario whose collider signature at the ILC with polarized beams was recently considered in ref. [10]. Briefly stated, in this scenario, the Higgs fields are considered to be the Nambu-Goldstone Bosons (NGB) of the non-linear realization of some global symmetry breaking.

In our numerical analysis for LHM, there are two free parameters f and θ_H. As argued by [15], precision electroweak measurements restrict the parameters to be $f \sim 1$ TeV and $0.1 < \cos\theta_H < 0.9$. In our study we consider a value of $f = 1$ TeV and $\cos\theta_H = 0.3$ satisfying these restrictions.

3 Analyses of $e^+e^- \to WW$

In this section we present the results of our numerical analysis to probe the Z' models through the process $e^+e^- \to WW$ at the ILC. This process gets an additional s-channel contribution through the exchange of the heavier gauge bosons, Z_2. Only the SM component of Z_2 interacts with W, and therefore this additional s-channel contribution is not present in the absence of mixing. At the same time, Z_1 becomes the SM gauge boson, Z^0 with the standard couplings, when there is no mixing. The t-channel with ν-exchange is not affected by new physics here as W interactions with SM fermions proceed through standard couplings. Thus the $e^+e^- \to WW$ process directly probes the $Z^0 - Z'$ mixing,

unlike processes like $e^+e^- \to f\bar{f}$, which gets contribution from the presence of Z' even when there is no mixing.

Thus for the process $e^+e^- \to W^+W^-$, we have an s-channel process with the exchange of the heavy neutral gauge boson, Z_2, in addition to the standard channels as shown in Fig. 1.

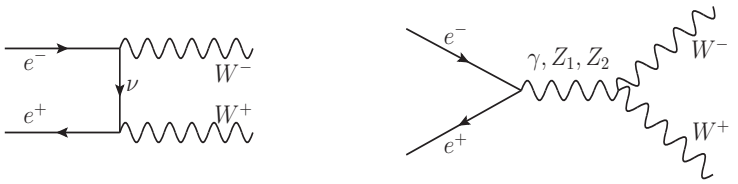

Figure 1: Feynman diagrams contributing to the process $e^+e^- \to W^+W^-$ in the Z' models.

The three-point gauge couplings involving WW are given by:

$$V^\mu(k_1)W^\nu(k_2)W^\rho(k_3) = ig_{VWW}\ [g^{\mu\nu}(k_1-k_2)^\rho + g^{\nu\rho}(k_2-k_3)^\mu + g^{\rho\mu}(k_3-k_1)^\nu]\,,$$

where all the momenta are considered outflowing, and $V \equiv \gamma,\ Z_1,\ Z_2$.

Direct search results from $p\bar{p}$ collisions at TeVatron as well as precision electroweak analysis constrain the parameters discussed in the previous section [5]. In most cases Z_2 mass slightly smaller than 1 TeV is permitted. This is translated into allowed range of couplings in a specific version of E_6 model as presented in Table 1. In our numerical studies we consider a conservative value of 0.003 and 100 MeV for the mixing angle and the parameter ΔM, respectively. The above parameter choices correspond to a Z_2 of mass ~ 1400 GeV .

For a non-exhaustive list of phenomenological studies of Z' in the context of LHC as well as ILC, see reference in [16, 17, 18, 19]. Previous phenomenological studies of $e^+e^- \to WW$ process in the context of Z' have considered different observables at the production level [14, 19], and have obtained the reach of ILC in probing the model. In this work our main focus is on various observables constructed with the decay products of the W's produced. One obvious advantage is that these observables do not require full reconstruction of the WW events, unlike in the former case. In this section, we will first report our analysis of the process at the production level with a study of the total cross section, and subsequently analyze different decay distributions and other observables.

3.1 The total cross section

We compute the total cross section incorporating beam polarization using the helicity amplitudes given in ref. [3] with the new couplings and with the added contribution due to the exchange of Z_2. With beam polarization, in general, the polarized cross section may be expressed as:

$$\sigma(e^+e^- \to W^+W^-) = \frac{1}{4}\left[(1+P_{e^-}).(1-P_{e^+})\sigma^{RL} + (1-P_{e^-}).(1+P_{e^+})\sigma^{LR}\right], \quad (11)$$

where $\sigma^{RL} = \sigma(e_L^+ e_R^- \to W^+W^-)$ and $\sigma^{LR} = \sigma(e_R^+ e_L^- \to W^+W^-)$, with $e_{L,R}$ representing the left- and right-polarized electrons (and positrons), respectively. The degree of polarization is defined as: $P_e = (N_R - N_L)/(N_R + N_L)$, where $N_{L,R}$ denote the number of left-polarized and right-polarized electrons (and positrons), respectively. More than 80% of electron beam polarization and large positron beam polarization are expected to be achieved at ILC. In our analysis we consider both the ideal possibility of 100% polarization along with the realistic polarization of the beams that will be achieved at ILC.

The models considered here are insensitive to the total cross section even at higher centre of mass energies. The inclusion of beam polarizations has no significant effect. In Table 3, we present the total production cross section for SM and Z' models considering both unpolarized and polarized beams. It can be seen that at $\sqrt{s}$=500 GeV, the deviation for different Z' models from the SM using unpolarized beams is about 0.05 - 0.3%. The deviation is slightly increased to about 0.7% at $\sqrt{s}$=800 GeV. Switching on the polarization with left-handed electrons and right-handed positrons it is seen that with this choice of polarization the cross section is about four times more than the unpolarized case. Although the deviation in this case follows the same pattern as the unpolarized one, but due to the larger size of the cross section $Z - Z'$ mixing can be studied more effectively. However with right-handed electrons and left-handed positrons, due to the absence of the dominant t channel the mixing effect is more pronounced, even though the cross section is very small compared to the other two cases. This particular combination thus leads to an increased signal by background ratio. It can be seen that the deviation is about 24% for different E_6 models and 50% for the LRSM and ALRSM model at $\sqrt{s}$=800 GeV, with 100% beam polarization. We have only presented the figure for this particular case. In Fig. 2 we present the total production cross-section in the case of SM and $E_6(\chi)$ as this has a maximum deviation compared to other E_6 models. Moreover, it can be seen that the percent deviation of LRSM and ALRSM are equal with this specific choice of beam polarization. LHM is also plotted for comparison. Since the gauge structure of LHM is different from the other Z' models considered here, it behaves differently from them. It is not much constrained compared to the other models as can be seen from Fig. 2. Taking into account the polarization which will be achieved at ILC, different E_6 models show about 4% deviation from the SM. The percent deviation for LRSM and ALRSM is about 9% compared to 50% obtained in the ideal case.

3.2 Double Energy Distribution

In order to exploit further the process at hand, it is profitable to consider the decays of one or both the W's. Let us consider $e^+e^- \to W^+W^-$ with both

P_e^-	P_e^+	model	$\sqrt{s}$ =300 GeV	$\sqrt{s}$ =500 GeV	$\sqrt{s}$ =800 GeV	$\sqrt{s}$ =1000 GeV
		SM	13.598	7.208	3.744	2.692
		$E_6(\chi)$	13.618	7.227	3.767	2.724
		$E_6(\psi)$	13.602	7.212	3.749	2.699
0	0	$E_6(\eta)$	13.612	7.223	3.762	2.717
		LRSM	13.601	7.212	3.750	2.701
		ALRSM	13.571	7.183	3.720	2.666
		LHM	13.679	7.347	3.867	2.973
		SM	53.973	28.716	14.940	10.746
		$E_6(\chi)$	54.042	28.777	14.994	10.798
		$E_6(\psi)$	54.005	28.743	14.963	10.767
-1	1	$E_6(\eta)$	54.038	28.774	14.991	10.795
		LRSM	54.013	28.753	14.981	10.800
		ALRSM	53.895	28.640	14.862	10.660
		LHM	54.214	29.205	15.362	11.796
		SM	41.023	21.826	11.355	8.167
		$E_6(\chi)$	41.076	21.871	11.396	8.206
		$E_6(\psi)$	41.048	21.845	11.372	8.183
-0.9	0.6	$E_6(\eta)$	41.073	21.869	11.393	8.204
		LRSM	41.053	21.850	11.376	8.187
		ALRSM	40.964	21.767	11.295	8.102
		LHM	41.208	22.198	11.676	8.966
		SM	0.418	0.114	0.037	0.023
		$E_6(\chi)$	0.427	0.122	0.045	0.030
		$E_6(\psi)$	0.401	0.103	0.028	0.015
1	-1	$E_6(\eta)$	0.411	0.110	0.034	0.020
		LRSM	0.390	0.093	0.018	0.003
		ALRSM	0.390	0.093	0.018	0.003
		LHM	0.500	0.182	0.105	0.096
		SM	0.857	0.374	0.178	0.125
		$E_6(\chi)$	0.865	0.381	0.184	0.131
		$E_6(\psi)$	0.845	0.365	0.171	0.119
0.9	-0.6	$E_6(\eta)$	0.853	0.371	0.176	0.123
		LRSM	0.837	0.360	0.167	0.115
		ALRSM	0.835	0.357	0.162	0.109
		LHM	0.922	0.431	0.233	0.191

Table 3: Total cross section (in pb) for different models with both polarized and unpolarized beams. The parameter used for LHM is f=1 TeV and c=0.3, and for the Z' models $\theta = 0.003$ and $\Delta M = 100$ MeV

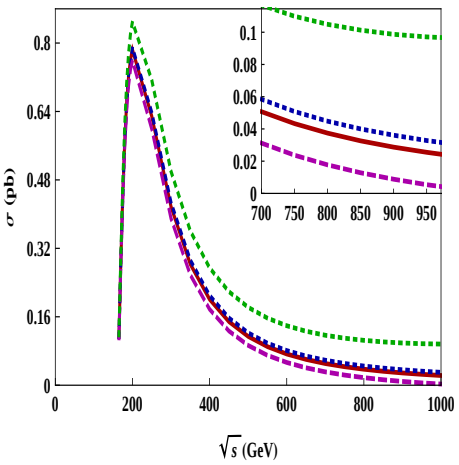

Figure 2: Total cross section for W^+ W^- production in an e^+e^- collision for SM[Red-Solid], ALRSM, LRSM [Magenta-Dashed], LHM [Green-Dotted] and $E_6(\chi)$ [Blue-Dotted] with polarized beams with P_{e^-}=1 and P_{e^+}=-1. For $U(1)'$ models, $\theta = 0.003$ and $\Delta M = 100$ MeV are considered. The parameter values of f=1 TeV and c=0.3 are used for LHM

W's decaying into leptons. The differential cross section in this case can be expressed as

$$\frac{d\sigma}{d\cos\Theta\ d\cos\theta^*_-\ d\phi^*_- d\cos\theta^*_+\ d\phi^*_+} = \frac{9\beta}{8192\pi^3 s} B(W^- \to l^-\bar{\nu}_l) B(W^+ \to l^+\nu_l) \mathcal{P}^{\lambda\bar{\lambda}}_{\lambda'\bar{\lambda}'} \mathcal{D}^{\lambda}_{\lambda'}\ \bar{\mathcal{D}}^{\bar{\lambda}}_{\bar{\lambda}'}, \tag{12}$$

where Θ is the scattering angle and $\beta = \sqrt{(1-4m_W^2/s)}$ is the velocity of the W in the centre of mass frame, $\sqrt{s}$ being the centre of mass energy. The other angles, $\theta^*_\mp$ and $\phi^*_\mp$ are the polar and azimuthal angles of the lepton/antilepton in the rest-mass frame of $W^\mp$ with boost direction of W^- along the z-axis, respectively. The production and decay tensors, $\mathcal{P}^{\lambda\bar{\lambda}}_{\lambda'\bar{\lambda}'}$, $\mathcal{D}^{\lambda}_{\lambda'}$ and $\bar{\mathcal{D}}^{\bar{\lambda}}_{\bar{\lambda}'}$ are given in [3]. The energy of the $l^\mp$ in the centre of mass frame is related to $\theta^*_\mp$ in the following way:

$$E_{l^\mp} = \frac{\sqrt{s}}{4}\ \left(1 \pm \beta\cos\theta^*_\mp\right), \tag{13}$$

This allows us to obtain the double energy differential cross section from Eq. 12 as

$$\frac{d\sigma}{dE_{l^-}dE_{l^+}} = \int \left(\frac{2}{\beta\gamma m_W}\right)^2 \frac{d\sigma}{d\cos\Theta\ d\cos\theta^*_-\ d\phi^*_- d\cos\theta^*_+\ d\phi^*_+}\, d\cos\Theta\ d\phi^*_-\ d\phi^*_+. \tag{14}$$

Following the notation of Dicus and Kallianpur [12], the energies of the leptons $E_{l^\pm}$ are expressed as dimensionless variables $X_{l^\pm}$ defined as:

$$X_{l^\pm} = \frac{2}{\beta\sqrt{s}}\left(E_{l^\pm} - \frac{\sqrt{s}}{4}(1-\beta)\right). \tag{15}$$

$X_{l^\pm}$ varies between 0 and 1. In Table 4 we present the percentage of events in bins of X_{l^-} and X_{l^+} obtained from

$$\frac{1}{\sigma}\frac{d^2\sigma}{dX_{l^+}dX_{l^-}}$$

at $\sqrt{s} = 800$ GeV using unpolarized beams. As expected in the case of SM the distribution peaks at maximum values of X_{l^-} and X_{l^+}. This behaviour dominates in other models as well. Since the matrix in Table 4 is symmetric under interchange of X_{l^-} and X_{l^+} (see Ref. [12] for explicit expression), we have shown only the upper half. We have numerically checked that the matrix is indeed symmetric.

A combination of the effects result in about 5% deviation in the case of $E_6(\chi)$ and ALRSM models, but with a qualitative difference. In the case of $E_6(\chi)$ it is an enhancement, whereas in the ALRSM case there is a reduction. The effect is reduced to smaller than 4% in the case of $E_6(\eta)$ model, while in the case of $E_6(\psi)$ and LRSM models it is a very negligible contribution of about 1%. The most sensitive bin in all the cases is the one with $0.2 \leq (X_{l^-}, X_{l^+}) \leq 0.4$, with about 0.6% of the total events in the case of SM. Such small deviation of a few percent is therefore hard to detect even at a high luminosity machine like the ILC. On the other hand, the LHM model, while showing similar qualitative behaviour, deviates from the SM value by about 34% in the same bin, leaving scope of detection at the ILC.

In the above analysis we have not made any attempt to optimize our results by considering different binning options. We expect the qualitative behaviour to remain more or less the same even in the optimal case. This is supported by Fig. 3 and Fig. 4, where we plot the double energy distribution for SM and the deviation from SM expressed as

$$\frac{\left.\frac{d^2\sigma}{dX_{l^-}dX_{l^+}}\right|_{model} - \left.\frac{d^2\sigma}{dX_{l^-}dX_{l^+}}\right|_{SM}}{\left.\frac{d^2\sigma}{dX_{l^-}dX_{l^+}}\right|_{SM}}.$$

We can see from Fig. 3 as discussed before, in the case of SM the distribution peaks at maximum values of X_{l^-} and X_{l^+}.

The use of right-handed electron beam and left-handed positron beam is expected to have a much larger sensitivity to all the models. In the case of LHM, while the new gauge boson do not contribute, owing to the fact that this does not couple to the right-handed electrons, the changed fermionic couplings of the SM gauge boson provides substantial effect [10]. In this case, the t-channel contribution is not present, and therefore both the SM as well as new

X_{l^-} \ X_{l^+}	0.2	0.4	0.6	0.8	1.0
1.0					
	0.428	2.705	7.174	13.837	22.693[a]
	0.433	2.707	7.174	13.773	22.566[b]
	0.429	2.705	7.170	13.824	22.665[c]
	0.431	2.707	7.159	13.788	22.594[d]
	0.429	2.706	7.170	13.823	22.664[e]
	0.422	2.702	7.197	13.907	22.832[f]
	0.465	2.716	7.023	13.386	21.804[g]
0.8					
	0.355	1.747	4.459	8.488	
	0.368	1.772	4.474	8.475	
	0.358	1.753	4.462	8.486	
	0.365	1.767	4.471	8.478	
	0.358	1.753	4.462	8.486	
	0.341	1.720	4.441	8.503	
	0.450	1.920	4.567	8.389	
0.6					
	0.364	1.053	2.418		
	0.379	1.087	2.452		
	0.367	1.060	2.425		
	0.376	1.080	2.445		
	0.367	1.060	2.426		
	0.348	1.016	2.381		
	0.475	1.293	2.657		
0.4					
	0.454	0.622			
	0.466	0.652			
	0.456	0.628			
	0.463	0.645			
	0.456	0.629			
	0.442	0.590			
	0.541	0.833			
0.2					
	0.626				
	0.628				
	0.626				
	0.628				
	0.626				
	0.623				
	0.646				

Table 4: Percentage of events at $\sqrt{s}$=800 GeV with unpolarized beams in bins of X_{l^-} and X_{l^+} corresponding to different models: a =SM, b=$E_6(\chi)$, c=$E_6(\psi)$, d=$E_6(\eta)$, e=LRSM, f=ALRSM and g=LHM. The parameters for $U(1)'$ models, θ=0.003 and δM=100 MeV, while for LHM $f = 1$ TeV and $c = 0.3$ are used

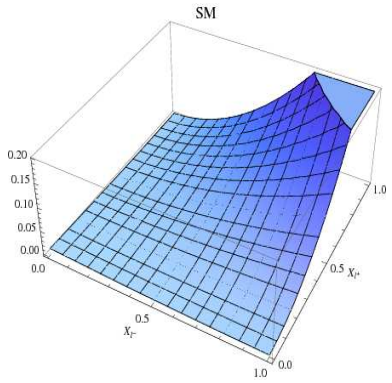

Figure 3: Double energy distribution for the SM at $\sqrt{s} = 800$ GeV with unpolarized beams

physics contributions show a symmetric behaviour. The difference in the two cases is, as expected, a constant shift, either positive or negative. At $\sqrt{s} = 800$ GeV, about 50% deviation is seen for both LRSM and ALRSM models, while $E_6(\psi)$ has about 40% deviation. The other two models show slightly reduced sensitivity with about 30% and 12% deviations in the case of $E_6(\chi)$ and $E_6(\eta)$ models respectively.

3.3 Single Energy Distribution

Energy distribution of the secondary lepton obtained by integrating the double energy distribution in Eqn. 14 over E_{l^+}, is another observable that might give

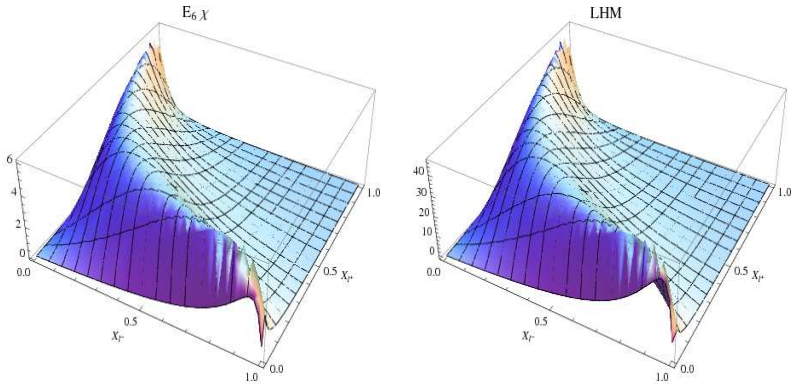

Figure 4: Double energy distribution showing the percentage deviation for the two models (a) $E_6(\chi)$ and (b) LHM from the SM at $\sqrt{s} = 800$ GeV with unpolarized beams. In the case of $E_6(\chi)$ $\theta = 0.003$ and $\Delta M = 100$ MeV, and in the case of LHM $f = 1$ TeV and $c = 0.3$ are used

a handle on the new effects. In Figs. 5, 6 we plot the energy distribution of the lepton for the case of $\sqrt{s}$ = 800 GeV for both ideal and realistic degrees of beam polarizations. The signs of the beam polarization are chosen so as to essentially switch off the SM t-channel contribution, so as to enhance the effects of the new physics. There is no appreciable deviation in the case of unpolarized beams (and in the case of left-handed electron beams). We notice that the LRSM and ALRSM cases behave qualitatively differently compared to the E_6 models and the LHM. While in the former case there is a reducing effect for the entire range of X_{l^-}, the latter has an increasing effect. This could be used as a discriminating factor between the left-right symmetric models and the other models used.

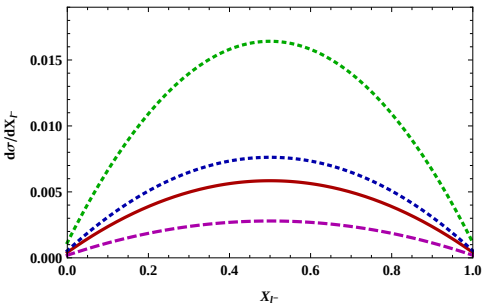

Figure 5: Energy distribution of the secondary leptons. with polarized beams with P_{e^-}=1 and P_{e^+}=-1 at $\sqrt{s}$ = 800 GeV. The parameters used are ΔM=100 MeV and θ=0.003 for $U(1)'$ type of models, and f = 1 TeV and c = 0.3 in the case of LHM. Different curves correspond to SM (Red-Solid), LHM (Green-Dotted), $E_6(\chi)$ (Blue-Dotted), and ALRSM and LRSM (Magenta-Dashed).

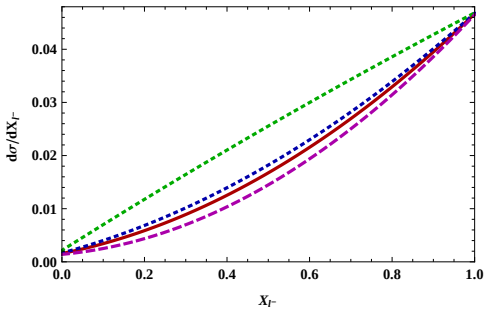

Figure 6: Energy distribution of the secondary leptons. with polarized beams with P_{e^-}=0.9 and P_{e^+}=-0.6 at $\sqrt{s}$ = 800 GeV. The parameters used are ΔM=100 MeV and θ=0.003 for $U(1)'$ type of models, and f = 1 TeV and c = 0.3 in the case of LHM. Different curves correspond to SM (Red-Solid), LHM (Green-Dotted), $E_6(\chi)$ (Blue-Dotted), and ALRSM and LRSM (Magenta-Dashed).

Note that in the case of realistic degrees of polarization since the neutrino t- channel effects are present, the panels comparing ideal and realistic degrees of freedom appear quite different as functions of X_{l^-}.

3.4 Angular Spectrum of the Secondary Lepton

We next consider the angular distribution of one of the secondary leptons. The way of calculating the angular distribution is done in our earlier work [10], which we follow here. The angular distributions for different polarization combinations in case of different models is calculated for $\sqrt{s}$ =800 GeV. As in the earlier cases, the case of unpolarized beams and the case of left-handed electron beams are not significant in the case of angular distribution as well. But the

case of right-handed polarization of electron beam along with the left handed polarization of the positron beam provides much better discrimination. This distribution is shown in the Figs. 7, 8 for both the ideal and realistic degrees of beam polarizations. Qualitatively, the picture as regards discrimination between the models, remains more or less the same as in the case of single energy distribution, except that there is a small difference between the two cases of left-right symmetric models considered. In the best case, the ALRSM model shows a deviation of around 45% for the parameter set used.

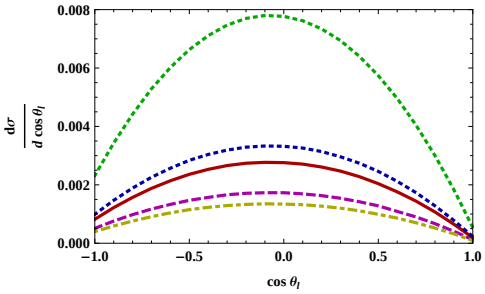

Figure 7: Angular distribution of one of the secondary leptons at $\sqrt{s}$=800 GeV using polarized beams with P_{e^-}=1 and P_{e^+}= -1 in the case of SM (Red-Solid), LHM (Green-Dotted), $E_6(\chi)$ (Blue-Dotted), ALRSM (Yellow-DotDashed) and LRSM (Magenta-Dashed). The parameters used are ΔM=100 MeV and $\theta = 0.003$ in the case of E_6 and LR models, and $f = 1$ TeV and $c = 0.3$ in the case of LHM.

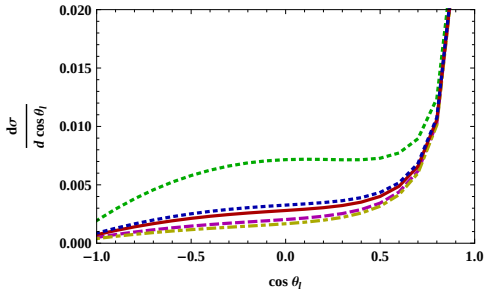

Figure 8: Angular distribution of one of the secondary leptons at $\sqrt{s}$=800 GeV using polarized beams with P_{e^-}=0.9 and P_{e^+}= -0.6 in the case of SM (Red-Solid), LHM (Green-Dotted), $E_6(\chi)$ (Blue-Dotted), ALRSM (Yellow-DotDashed) and LRSM (Magenta-Dashed). The parameters used are ΔM=100 MeV and $\theta = 0.003$ in the case of E_6 and LR models, and $f = 1$ TeV and $c = 0.3$ in the case of LHM..

Fig. 8 shows the forward-backward asymmetric behaviour arising from the Zee coupling, which is different for different models considered. With this observation, we may obtain the fraction of leptons emitted in the backward direction, which may be defined as

$$f_{back} = \frac{\int_{-1}^{0} (d\sigma/d\cos\theta_l)\ d\cos\theta_l}{\int_{-1}^{1} (d\sigma/d\cos\theta_l)\ d\cos\theta_l}.$$

This fraction is a useful quantity to consider in the case of unpolarized and left-polarized electron beams as well. In Table 5 we present these fractions for $\sqrt{s}$ = 500 GeV, 800 GeV and 1000 GeV. The result shows with unpolarized beams about 3-4 % of the leptons are emitted in the backward hemisphere. The deviation is about 3% in going from SM to $E_6(\chi)$ and ALRSM which are more sensitive compared to other models. At $\sqrt{s}$=800 GeV, the deviation becomes more significant and is about 8%. However LHM being more sensitive shows $\sim$ 36 % deviation at $\sqrt{s}$=500 GeV which further increases with energy. This

above results are slightly increased by switching on the beam polarization to left-handed electrons and right-handed positrons. The departure from ideal degrees of polarization does not play a significant role at the level of significant places retained in the tables for this configuration.

We see from Table 5 that for the case of polarization with about 90% of right handed electrons and 60% of left handed positrons, the deviation increases. Owing to the near absence of the dominant t- channel neutrino diagram with this polarization configuration, the new physics contribution shows up in the fraction of the leptons emitted in the backward direction. Thus at $\sqrt{s}$= 800 GeV for $E_6(\psi)$ and $E_6(\chi)$ there is about 15% deviation from SM, whereas $E_6(\eta)$ is more constrained with only 5% deviation. The symmetric models ALRSM and LRSM are more sensitive with about 30% deviation.

In the case of completely right handed electrons and left handed positrons, from the same table it may be seen that all the models give rise to the same prediction as the SM. This is a consequence of the near symmetric behaviour in the angular distributions as shown in Fig. 7. Due to this property the new physics effects in f_{back} and A_{FB} are essentially wiped out. It is important to note that this feature persists with completely right-polarized electron and partially left-polarized positrons, and *vice versa*.

Another useful observable related to the angular asymmetry is the forward-backward asymmetry defined as

$$A_{FB} = \frac{\int_{-1}^{0}(d\sigma/d\cos\theta_l)\ d\cos\theta_l - \int_{0}^{1}(d\sigma/d\cos\theta_l)\ d\cos\theta_l}{\int_{-1}^{1}(d\sigma/d\cos\theta_l)\ d\cos\theta_l}. \tag{16}$$

The values for this asymmetry is also presented in Table 5 for different models at three different collider energies. This asymmetry shows a similar behaviour as that of the fraction of the leptons emitted in the backward direction as regards the beam polarization configurations and discrimination between the models. In fact, the two observables are intimately related: $A_{FB} = 2f_{back} - 1$. However, since they are experimentally realized differently, it may be appropriate to consider both of them.

3.5 Left-Right Asymmetry

The left-right asymmetry is another important observable to be considered for studying the new models. We define the left-right asymmetry in the differential cross section as:

$$A_{LR}^{diff} = \frac{d\sigma(e_R^+e_L^-)/d\cos\theta - d\sigma(e_L^+e_R^-)/d\cos\theta}{d\sigma(e_R^+e_L^-)/d\cos\theta + d\sigma(e_L^+e_R^-)/d\cos\theta}, \tag{17}$$

where θ is the W scattering angle.

The Z' of the $U(1)'$ models considered here couples to both left- and right-handed fermions, but with varying relative couplings. Thus, one would expect appreciable change in the asymmetry between the left- and right-polarized cross

P_{e^-}	P_{e^+}	Model	$\sqrt{s}$ =500GeV		$\sqrt{s}$ =800GeV		$\sqrt{s}$ =1000GeV	
			f_{back}	A_{FB}	f_{back}	A_{FB}	f_{back}	A_{FB}
0	0	SM	0.0346	-0.9308	0.0238	-0.9524	0.0208	-0.9585
		$E_6(\chi)$	0.0356	-0.9288	0.0257	-0.9487	0.0234	-0.9532
		$E_6(\psi)$	0.0347	-0.9305	0.0242	-0.9517	0.0213	-0.9574
		$E_6(\eta)$	0.0353	-0.9293	0.0252	-0.9496	0.0228	-0.9545
		LRSM	0.0347	-0.9306	0.0241	-0.9517	0.0213	-0.9573
		ALRSM	0.0330	-0.9339	0.0208	-0.9585	0.0161	-0.9677
		LHM	0.0474	-0.9053	0.0474	-0.9052	0.0212	-0.9574
-0.9	0.6	SM	0.0324	-0.9353	0.0225	-0.9550	0.0197	-0.9606
		$E_6(\chi)$	0.0332	-0.9335	0.0241	-0.9518	0.0219	-0.9561
		$E_6(\psi)$	0.0327	-0.9345	0.0232	-0.9537	0.0206	-0.9588
		$E_6(\eta)$	0.0332	-0.9336	0.0240	-0.9520	0.0218	-0.9563
		LRSM	0.0328	-0.9343	0.0233	-0.9533	0.0209	-0.9583
		ALRSM	0.0312	-0.9376	0.0201	-0.9598	0.0160	-0.9681
		LHM	0.0440	-0.9120	0.0441	-0.9118	0.0167	-0.9666
0.9	-0.6	SM	0.1618	-0.6765	0.1061	-0.7878	0.0909	-0.8183
		$E_6(\chi)$	0.1694	-0.6612	0.1208	-0.7583	0.1116	-0.7788
		$E_6(\psi)$	0.1518	-0.6964	0.0889	-0.8222	0.0680	-0.8639
		$E_6(\eta)$	0.1587	-0.6826	0.1013	-0.7975	0.0845	-0.8310
		LRSM	0.1457	-0.7087	0.0786	-0.8427	0.0552	-0.8896
		ALRSM	0.1426	-0.7148	0.0648	-0.8703	0.0268	-0.9463
		LHM	0.2174	-0.5653	0.2120	-0.5760	0.2251	-0.5498
1	-1	All models	0.5834	0.1668	0.5392	0.0785	0.5264	0.0528

Table 5: Fraction of leptons emitted in the backward direction, and the forward-backward asymmetry for all models for unpolarized and polarized beams with a parameter choice of θ=0.003 and ΔM= 0.1 GeV. The parameters for LHM are f=1 TeV and c=0.3

sections. But compared to these the new gauge boson in the LHM has the peculiar property of coupling only to left-handed fermions as mentioned earlier.

Fig. 9(a) shows the LR asymmetry for $\sqrt{s}$=800 GeV. Even at low energies the deviation becomes apparent. Notice also that the LHM now pair with the left-right symmetric models unlike in the case of energy and angular distributions shown in Figures 5 and 7, providing us another tool for discriminating different models from each other.

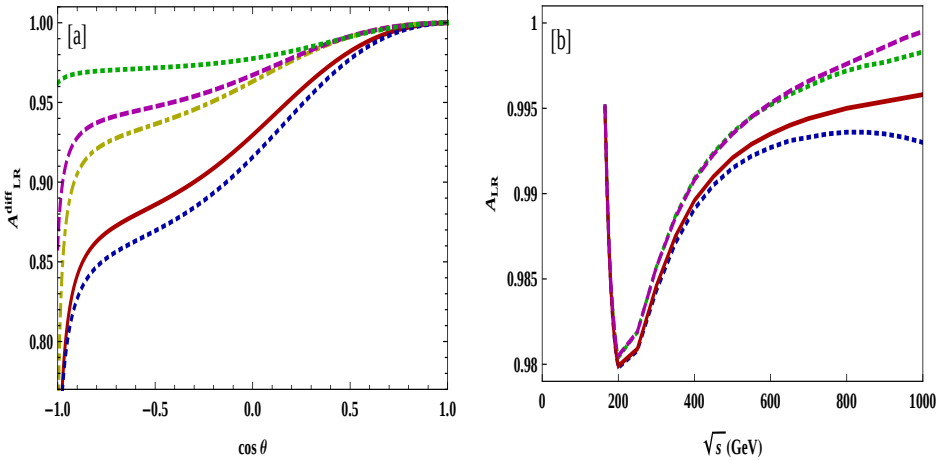

Figure 9: (a) Differential Left-right asymmetry as a function of the scattering angle for different models at $\sqrt{s}$ = 800 GeV, and (b) the integrated left-right asymmetry as a function of the centre of mass energy for different models: SM (Red-Solid), LHM(Green-Dotted), $E_6(\chi)$ (Blue-Dotted), LRSM(Magenta-Dashed) and ALRSM (Yellow-DotDashed). Parameters used are $\theta = 0.003$ and $\Delta M = 100$ MeV for the E_6 and LR models, and $f = 1$ TeV and $c = 0.3$ for the LHM.

We may go one step further by considering an integral version of this asymmetry as better efficiency may be obtained this way, by integrating each of the differential cross sections from an opening angle θ_0 up to an angle $\pi - \theta_0$, for various realistic values of θ_0 to which the data can be integrated without difficulty. We define the integrated left-right asymmetry as:

$$A_{LR} = \frac{\sigma_{\theta_0}(e^+_R e^-_L \to WW) - \sigma_{\theta_0}(e^+_L e^-_R \to WW)}{\sigma_{\theta_0}(e^+_R e^-_L \to WW) + \sigma_{\theta_0}(e^+_L e^-_R \to WW)} \tag{18}$$

where σ_{θ_0} stands for $\int_{\theta_0}^{\pi-\theta_0} (d\sigma/d\theta)\ d\theta$.

This asymmetry, for different parameter models is plotted against the centre of mass energy in Fig. 9(b) with θ_0 =0. Dominance of the t-channel in the W-pair production establishes a highly forward peaked cross section, whereas as is seen from Fig. 9(a) the deviations in LR asymmetry grows with the scattering angle, except for a region near $\theta = 180$ degrees. Thus, the cut-off angle

can be effectively used to increase the deviation in the asymmetry. The results are presented in Table 6 for different cut off angles in different models at different centre of mass energies. An asymmetric cut off, meaning and integrated asymmetry between scattering angles, θ_{10} and $\pi - \theta_{20}$, with $\theta_{20} \neq \theta_{10}$, may improve the situation quantitatively. Again, as in the case of other observables, our gaol in this report is to demonstrate the viability of identifying deviations from the SM case, and further providing tools to disentangle different possible models. With this illustrative purpose in mind, we do not attempt to optimize the investigation.

4 Discussion and Conclusions

In the present work we have considered a class of additional Z' models which are of interest to the linear collider community, both at the ILC as well as at CLIC. While the masses of these bosons are already required to be significantly high, their imprint through mixing with the standard model Z boson is the subject of this investigation. By considering popular E_6 and left-right symmetric models like LRSM and ALRSM we have demonstrated that the new physics signatures due to these models can be imprinted only at higher center of mass energies. In the LHM model considered in our earlier work [10], Z' had the property of coupling only to left-handed fermions. This is in contrast to the other models considered here where Z' behaves like the SM Z. Thus compared to LHM, these models do not show appreciable deviation at lower center of mass energies.

While our focus in W-pair production at ILC is on the unambiguous signal that it provides for $Z_{SM} - Z'$ mixing, we notice the interesting possibility of model discrimination here. For example, let us compare the deviations of some of the observables from their SM values. In the case of energy and angular momentum distributions notice the qualitatively different behaviour of left-right symmetric models compared to E_6 models and LHM. Similarly, in the case of integrated and differential left-right asymmetries the E_6 model has a different qualitative behaviour compared to the LHM and left-right symmetric models.

Note that WWZ_i $(i = 1, 2)$ coupling is insensitive to differences between Z' models, and therefore it is the coupling of Z' with the initial electron and positron that enables any possible model discrimination in the present case. Thus, one would imagine that fermion pair production process is better suited to distinguish different models. In a recent study, the potential of the ILC to discriminate between Z' models through fermion pair production is studied in Ref. [16]. Here the sensitivity is studied by considering cross sections which are shown to be sensitive to new physics due to the availability of high statistics at the ILC. It is also shown that beam polarization does enhance the sensitivity in an essential manner. Similar studies with Drell-Yan dilepton production [17] also probe distinguishability of different Z' models at LHC. At the same time, our study indicates that W-pair production at ILC is capable of supplementing the fermion pair production process in model discrimination in the case of Z' models. More extensive analysis involving a parameter scan, also incorporating a realistic

Cut off angle θ_0	Model	A_{LR}		
		$\sqrt{s}$=500GeV	$\sqrt{s}$= 800 GeV	$\sqrt{s}$= 1000 GeV
0	SM	0.9921	0.9950	0.9958
	$E_6(\chi)$	0.9914	0.9936	0.9930
	$E_6(\psi)$	0.9930	0.9967	0.9984
	$E_6(\eta)$	0.9924	0.9956	0.9968
	LRSM	0.9935	0.9976	0.9995
	ALRSM	0.9935	0.9976	0.9995
	LHM	0.9945	0.9972	0.9983
15	SM	0.9853	0.9872	0.9877
	$E_6(\chi)$	0.9842	0.9836	0.9800
	$E_6(\psi)$	0.9870	0.9916	0.9955
	$E_6(\eta)$	0.9860	0.9889	0.9909
	LRSM	0.988	0.9939	0.9985
	ALRSM	0.9879	0.9938	0.9985
	LHM	0.9885	0.9933	0.9956
30	SM	0.9742	0.9765	0.9771
	$E_6(\chi)$	0.9723	0.9703	0.9638
	$E_6(\psi)$	0.9772	0.9846	0.9917
	$E_6(\eta)$	0.9755	0.9797	0.9834
	LRSM	0.979	0.9889	0.9973
	ALRSM	0.9787	0.9885	0.9971
	LHM	0.9808	0.9890	0.9928
45	SM	0.9601	0.9622	0.9628
	$E_6(\chi)$	0.9574	0.9531	0.9434
	$E_6(\psi)$	0.9648	0.9753	0.9866
	$E_6(\eta)$	0.9622	0.9679	0.9738
	LRSM	0.9676	0.9822	0.9956
	ALRSM	0.9669	0.9811	0.9951
	LHM	0.9721	0.9845	0.9899
60	SM	0.9453	0.9466	0.9470
	$E_6(\chi)$	0.9418	0.9348	0.9224
	$E_6(\psi)$	0.9517	0.9652	0.9811
	$E_6(\eta)$	0.9483	0.9552	0.9638
	LRSM	0.9555	0.9750	0.9939
	ALRSM	0.9542	0.9727	0.9927
	LHM	0.9640	0.9807	0.9875

Table 6: Left-right asymmetry for different cut-off angles at selected $\sqrt{s}$ values for different models considered with a parameter choice of θ=0.003 and ΔM= 0.1 GeV. The parameters for LHM are f=1 TeV and c=0.3

collider-detector simulation is required to draw conclusions regarding ability of W-pair production in model discrimination at ILC, adapting the procedure in Ref. [16]. Alternatively one may contemplate adapting different asymmetries of the type we have proposed for fermion pair production as well. Perhaps a joint analysis involving both fermion pair production and W-pair production is needed to bring out the full potential of ILC in this regard.

Our conclusions for our models is as follows: we have studied in detail each of the E_6 models denoted by χ, ψ and η and the LRSM and ALRSM models. We find that at a centre of mass energy of 800 GeV, all these models show a sharp deviation from the SM predictions for energy-energy, single-energy and angular correlations of the decay lepton(s) generally for right-handed electron and left-handed positron with realistic degrees of polarization. Curiously for ideal polarization the decay lepton fraction and A_{FB} are insensitive to new physics for the same configuration above, as the t- channel contribution is totally absent in this case. The χ, LRSM and ALRSM models are more sensitive than the other models even with unpolarized beams. The reason for the absence of sensitivity at lower energies is due to the stringent bounds already present on the parameters of the models. The FB and LR asymmetries have also been studied, with the latter being more sensitive to new physics in all the models. These models remain less sensitive than the LHM model studied earlier. Any indication of $U(1)'$ type of Z' in W-pair production at ILC is a clear signal of $Z_{SM} - Z'$ mixing. Apart from this, the present study points to the potential of this process to supplement the fermion pair production process in model discrimination, through a suitable combination of observables considered.

Overall a strong polarization program at the ILC will significantly enhance the diagnostic capability towards additional Z' bosons particularly at higher design energies.

Acknowledgments: BA thanks the Department of Science and Technology, Government of India and the Homi Bhabha Fellowships Council for support during the course of these investigations. MP thanks the Department of Physics, Indian Institute of Technology Guwahati for hospitality when part of this work was done. PP thanks BRNS, DAE, Government of India for support through a project (**No.**: 2010/37P/49/BRNS/1446).

References

[1] J. Brau *et al.* [ILC Collaboration], arXiv:0712.1950 [physics.acc-ph].
G. Aarons *et al.* [ILC Collaboration], arXiv:0709.1893 [hep-ph].

[2] G. Moortgat-Pick *et al.*, Phys. Rept. **460**, 131 (2008) [arXiv:hep-ph/0507011].

[3] K. Hagiwara, R. D. Peccei, D. Zeppenfeld and K. Hikasa, Nucl. Phys. B **282**, 253 (1987).

[4] G. Gounaris, J. Layssac, G. Moultaka and F. M. Renard, Int. J. Mod. Phys. A **8**, 3285 (1993).

[5] K. Nakamura *et al.* [Particle Data Group], J. Phys. G **37**, 075021 (2010).

[6] T. Aaltonen *et al.* [CDF Collaboration], Phys. Rev. Lett. **102**, 091805 (2009) [arXiv:0811.0053 [hep-ex]].

[7] M. Jaffre [CDF and D0 Collaboration], PoS E **PS-HEP2009**, 244 (2009) [arXiv:0909.2979 [hep-ex]].

[8] J. Alcaraz *et al.* [The LEP Collaborations ALEPH, DELPHI, L3, OPAL, and the LEP Electroweak Working Group], arXiv:hep-ex/0612034.

[9] J. Erler, P. Langacker, S. Munir and E. R. Pena, JHEP **0908** (2009) 017 [arXiv:0906.2435 [hep-ph]].

[10] B. Ananthanarayan, M. Patra and P. Poulose, JHEP **0911**, 058 (2009) [arXiv:0909.5323 [hep-ph]].

[11] E. Accomando *et al.* [CLIC Physics Working Group], arXiv:hep-ph/0412251.

[12] D. A. Dicus and K. Kallianpur, Phys. Rev. D **32**, 35 (1985).

[13] P. Langacker, Rev. Mod. Phys. **81**, 1199 (2009) [arXiv:0801.1345 [hep-ph]].

[14] A. A. Pankov and N. Paver, Phys. Rev. D **48**, 63 (1993).

[15] A. Dobado, L. Tabares-Cheluci, S. Penaranda and J. R. Laguna, Eur. Phys. J. C **66**, 429 (2010) [arXiv:0907.1483 [hep-ph]].

[16] P. Osland, A. A. Pankov and A. V. Tsytrinov, Eur. Phys. J. C **67**, 191 (2010) [arXiv:0912.2806 [hep-ph]].

[17] P. Osland, A. A. Pankov, N. Paver and A. V. Tsytrinov, arXiv:1012.1456 [hep-ph];

P. Osland, A. A. Pankov, A. V. Tsytrinov and N. Paver, Phys. Rev. D **79** (2009) 115021 [arXiv:0904.4857 [hep-ph]].

[18] E. Accomando, A. Belyaev, L. Fedeli, S. F. King and C. Shepherd-Themistocleous, arXiv:1010.6058 [hep-ph];

E. Ramirez Barreto, Y. A. Coutinho and J. Sa Borges, Phys. Lett. B **689**, 36 (2010) [arXiv:1004.3269 [hep-ph]];

T. G. Rizzo, arXiv:0808.1906 [hep-ph];

T. G. Rizzo, arXiv:hep-ph/0610104;

K. Y. Lee, S. C. Park, H. S. Song and C. Yu, Phys. Rev. D **63**, 094010 (2001) [arXiv:hep-ph/0011173].

[19] A. A. Pankov and N. Paver, Phys. Lett. B **393**, 437 (1997) [arXiv:hep-ph/9610509].